Received: 12 April 2016 | Revised: 29 January 2017 | Accepted: 23 April 2017

DOI: 10.1002/ajpa.23243

TECHNICAL NOTE

WILEY American Journal of PHYSICAL ANTHROPOLOGY

New methodology to reconstruct in 2-D the cuspal enamel of modern human lower molars

Mario Modesto-Mata[1,2] | Cecilia García-Campos[1,3] | Laura Martín-Francés[1,3] | Marina Martínez de Pinillos[1,3] | Rebeca García-González[4] | Yuliet Quintino[4] | Antoni Canals[2,5,6] | Marina Lozano[5] | M. Christopher Dean[7] | María Martinón-Torres[3,4] | José María Bermúdez de Castro[1,3]

[1]Centro Nacional de Investigación sobre la Evolución Humana (CENIEH), Burgos 09002, Spain

[2]Equipo Primeros Pobladores de Extremadura, Casa de la Cultura Rodríguez Moñino, Cáceres, Spain

[3]Anthropology Department, University College London, London, UK

[4]Laboratorio de Evolución Humana, Área de Paleontología, Dpto. de Ciencias Históricas y Geografía, Universidad de Burgos, Burgos, Spain

[5]IPHES Institut Català de Paleoecologia Humana i Evolució Social, C/Marcel.lí Domingo s/n, Campus Sescelades URV (Edifici W3), Tarragona 43007, Spain

[6]Àrea de Prehistòria Universitat Rovira i Virgili (URV), Tarragona 43002, Spain

[7]Department of Cell and Developmental Biology, University College London, London, UK

Correspondence
Mario Modesto-Mata Centro Nacional de Investigación sobre la Evolución Humana (CENIEH), Paseo Sierra de Atapuerca 3, 09002 Burgos, Spain.
Email: paleomariomm@gmail.com

This article was published online on 15 May 2017. After online publication, minor revisions were made to the text. This notice is included in the online and print versions to indicate that both have been corrected on 26 May 2017.

Abstract

Objectives: In the last years different methodologies have been developed to reconstruct worn teeth. In this article, we propose a new 2-D methodology to reconstruct the worn enamel of lower molars. Our main goals are to reconstruct molars with a high level of accuracy when measuring relevant histological variables and to validate the methodology calculating the errors associated with the measurements.

Methods: This methodology is based on polynomial regression equations, and has been validated using two different dental variables: cuspal enamel thickness and crown height of the protoconid. In order to perform the validation process, simulated worn modern human molars were employed. The associated errors of the measurements were also estimated applying methodologies previously proposed by other authors.

Results: The mean percentage error estimated in reconstructed molars for these two variables in comparison with their own real values is −2.17% for the cuspal enamel thickness of the protoconid and −3.18% for the crown height of the protoconid. This error significantly improves the results of other methodologies, both in the interobserver error and in the accuracy of the measurements.

Conclusions: The new methodology based on polynomial regressions can be confidently applied to the reconstruction of cuspal enamel of lower molars, as it improves the accuracy of the measurements and reduces the interobserver error. The present study shows that it is important to validate all methodologies in order to know the associated errors. This new methodology can be easily exportable to other modern human populations, the human fossil record and forensic sciences.

KEYWORDS

molar reconstruction, polynomial regression, cuspal enamel thickness, crown height

1 | INTRODUCTION

Unworn teeth are important to assess crown formation times and enamel extension rates with a high degree of accuracy. Especially, an intact protoconid is of particular interest in developmental studies because it is the first cusp to start forming and the cusp that normally takes the longest time to finish its growth in molars (Mahoney, 2008). Unfortunately, the presence of unworn teeth in the fossil record is relatively scarce. The present study proposes a new methodology to reconstruct the protoconid of slightly worn lower molars, in order to increase of the number of samples where developmental variables could be evaluated. We employed the computerized microtomography

(microCT) technique, which has enabled the acquisition of many high-resolution virtual sections of fossil teeth. Variables that were previously inaccessible are now available, and the accuracy of the measurements has been significantly improved (Grine, 2005; Kono, 2004; Kono & Suwa, 2005; Macchiarelli et al., 2006; Martínez de Pinillos et al., 2014; Olejniczak & Grine, 2006; Olejniczak et al., 2007, 2008a, Olejniczak, Tafforeau, Feeney, & Martin, 2008b; Benazzi et al., 2014; Xing, Martinón-Torres, Bermúdez de Castro, Wu, & Liu, 2015).

Cuspal enamel thickness and crown height are two variables that are particularly affected by wear, and they are commonly employed, among others, to estimate enamel formation times. Thus, the obtention of a statistically controlled methodology to reconstruct the enamel would significantly help in estimating enamel formation times.

The enamel of teeth covers the crown from the cusp to the cervix, and has previously been divided into two continuous regions depending on whether long-period incremental lines within the enamel reach the surface (lateral enamel) or not (cuspal enamel) (FitzGerald & Rose, 2008; Hillson, 1996; Nanci, 2007). Crown formation time can therefore be calculated by summing cuspal enamel formation time with lateral enamel formation time. When this method of estimating total crown formation is adopted, different methodologies are required to estimate cuspal and lateral enamel formation times.

Cuspal enamel thickness is one useful measurement that has been employed to estimate cuspal enamel formation times (Dean et al., 2001; Mahoney, 2008). It has been defined as the linear distance between the tip of the dentine horn and the outer enamel surface at the point coincident with the first perikyma (Reid & Dean, 2006; Reid, Guatelli-Steinberg, & Walton, 2008; Smith et al., 2010). Estimating the time and rate of lateral enamel formation can be done using total counts of perikymata on the tooth surface or of long period incremental markings within the enamel from histological sections of teeth. In studies that compare teeth within and between individuals, it has become customary to divide the crown height into equal proportions or quantiles (usually deciles) to scale for differences in absolute crown height. Crown height of the protoconid is defined as the linear distance between the cusp tip of the enamel to the cemento-enamel junction (Reid & Dean, 2006). The number of perikymata can be counted and compared among deciles of crown height from cusp to cervix. The relative change in perikymata spacing, or packing pattern, among deciles can provide some kind of estimate of enamel extension rates (the rate at which ameloblasts differentiate along the enamel dentine junction during tooth formation). When periodicity (the number of days of enamel formation between perikymata) is known, the total number of perikymata can be used to estimate lateral enamel formation times (Guatelli-Steinberg & Reid, 2008).

In order to maximize available samples to make comparisons between species and populations, different methods of reconstructing worn molars have been described in the last few years. On the one hand, a reconstruction of worn surfaces has been conducted by following the contour of each side of the tooth cusp and projecting them toward the cusp tip until both sides meet (Guatelli-Steinberg & Reid, 2008). Here we refer to this method as Method 1. On the other hand, reconstructions of worn teeth have been based on the profiles of unworn ones of the same type (Smith et al., 2012). We refer to this method as Method 2. However, these methodologies have not been thoroughly described, thus the exact protocols remain unknown. Moreover, neither of these methods has been tested and/or validated, and so any errors in estimating cuspal formation times or enamel:dentine ratios from utilizing these reconstructions protocols is unknown. Some authors have criticized these studies that have not validated their methods (Benazzi et al., 2014), and others have emphasised the importance of validating the methodologies (Saunders, Chan, Kahlon, Kluge, & FitzGerald, 2007). The only author who developed and validated a reconstruction methodology was Saunders et al. (2007).

The main goal of this study was to present a new methodology to reconstruct slightly worn first and second lower permanent molars cusp (protoconid) by means of microCT images. A validation of this new methodology is also presented, as well as a comparative study applying the previous techniques (Methods 1 and 2).

2 | MATERIALS AND METHODS

2.1 | Materials

A total of 26 lower molars (M_1 = 10, M_2 = 16) were included in this study, belonging to different historic and archaeological modern human populations from the Iberian Peninsula (Table 1 and Figure 1): 14 individuals from the medieval churchyard of San Pablo (Burgos), four from the archaeological sites of Maltravieso Cave and one from Santa Ana Cave (both in Cáceres), four individuals of Galls Carboners Cave (Tarragona), two from Guineu Cave (Barcelona), and one from El Mirador Cave (Burgos, Spain). None of these teeth displayed any evidence of wear (category of wear stage 1, according to Molnar (1971)).

The comparative sample from San Pablo (Burgos) consists of a medieval churchyard and archaeological collection (XII–XIV) from the Dominican monastery of San Pablo housed in the Laboratory of Human Evolution at the University of Burgos (Spain).

Maltravieso Cave is located in Cáceres (Extremadura, Spain), in the southwestern part of the Iberian Peninsula. The cave was accidentally discovered in 1951 in a limestone quarry. The affected area was called Sala del Descubrimiento. In this room a thousand ceramic and human remains that were part of a collective grave were uncovered (Callejo,

TABLE 1 Number of M1s and M2s used in this study, divided by site and population

Site	M_1	M_2	Total
San Pablo churchyard	8	6	14
Maltravieso Cave	1	3	4
Santa Ana Cave	–	1	1
Galls Carboners Cave	1	3	4
Guineu Cave	–	2	2
El Mirador cave	–	1	1
Total	10	16	26

FIGURE 1 Map of the Iberian Peninsula with the location of the sites

1958). The few pottery fragments available indicate that the room was used as a burial cave at least in the half of the second millennium BC (Cerrillo & González, 2007). In 2002, various mechanical and manual test pits were performed in the area originally occupied by the Sala del Descubrimiento, uncovering new 172 remains belonging to *Homo sapiens* and several new pottery fragments (Muñoz & Canals, 2008). All of this new remains were assigned to be part of the assemblage discovered in the 1950s.

Santa Ana Cave presents several stratigraphical units that correspond to the Pleistocene (Carbonell et al., 2005). All the remains from the Pleistocene sediments were unconvered in a calcified breccia. However, sediments from historical ages have also been found, including Ancient Rome evidences. Although the exact historical period of the molar remains unknown, its attribution to *H. sapiens* is unquestioned.

Galls Carboners Cave is located in the Prades Mountains (Tarragona, Spain). A collective burial was excavated in different periods, the first in 1970s and then again in 2009 and 2010. Along with human remains (an NMI of 16 individuals) some lithic tools were recovered, as well as some ceramic fragments and faunal remains. The dating of a human remain places this site in 3,310 ± 30BP (Cal BP 3,620–3,460).

Guineu Cave is located in Font-Rubí (Barcelona, Spain). In this site, a long sequence with occupations ranging from hunter-gatherer to Bronze Age populations has been documented. In the 4th and 3rd millineum BC the cave was used as a burial place (Morales, Cebrià, Mestres, Oms, & Allué, 2013). The teeth used in this paper belong to this period. Some dated human remains shows an age about 2,871–3,353 Cal BC.

El Mirador Cave is located on the southern side of the Sierra de Atapuerca (Burgos, Spain). The human assemblage where this tooth belongs to is a collective burial found in an about 14 m^2 natural chamber located in the NE corner of the cave. Although there are some individuals in their original anatomical position, the superficial remains were mixed and disturbed by the actions of the clandestine excavators in the 1980s. Up to now, there are a minimum number of 22 individuals of different sexes and ages (Gómez-Sánchez et al., 2014). All of these human remains belong to the Chalcolithic period and have been dated to 4,760–4,200 years cal. BP.

For our study, one antimere per individual was selected. The inclusion criteria were the presence of the complete crown, good preservation and the absence of fractures or dental pathologies. The teeth were microCT using a Phoenix v/tome/x s of GE Measurement system, housed at the National Human Evolution Research Centre (CENIEH, Burgos, Spain) with the following scan settings: voltage 100 kV, 100 mA, 0.02 cooper filter and resultant isometric voxel size ranging from 18 (isolated dental remains) to 75 (mandibles) microns. MicroCT images were processed employing the software AMIRA 6.0.0 (Visage Imaging, Inc.).

2.2 | Description of the new methodology

2.2.1 | Reference plane

The plane of reference used to reconstruct the lower molars has been defined by Benazzi et al. (2014). Briefly summarized, the cervical plane is obtained as the best-fit plane among 50 equidistant landmarks located on the cemento-enamel junction. Then, the reference plane is created perpendiculary to the cervical plane, crossing through the two mesial dentine horns. The protoconid was situated to the right of the reference plane in order to standardize all of them. An example of the reference plane of one molar used in this study can be seen in Figure 2a.

2.2.2 | Outline of enamel and relative coordinates

We used the open-source software Inkscape 0.91 to convert the plane of reference into a vector graphic, using the raster-to-vector conversion (supporting information Text S1). In this way, the outline of the enamel was traced (Figure 2b).

We are interested in one particular area of the outline of the enamel, which was used to reconstruct the protoconid and is named here as POL-PR, which means POLynomial of the PRotoconid (Figure 2c). The outlines of the protoconids were used to generate a polynomial regression equation based on the relative coordinates of their points (from 0 to 100). The specific description of how to obtain these points and their coordinates in each area is described below.

The Cartesian coordinate system is defined by three landmarks (green dots in Figure 2c). The first landmark is the origin and is placed at the top of the dentine horn tip of the protoconid. The relative coordinates of the first landmark are (0,0). The second landmark is placed at the point where a horizontal line from the origin crosses the buccal aspect of the enamel of the protoconid. The coordinates of this second landmark are (100,0) and the distance between both landmarks is named *Xprotoconid*. The third landmark is located at the point where a horizontal line drawn from the highest point of the enamel cusp tip crosses the vertical line traced from the origin. The coordinates of this third landmark are (0,100) and the distance with the origin is named *Yprotoconid*. We placed 51 equidistant points over the outline of the protoconid between the second and third landmark (supporting information Text S2), and calculated their relative coordinates (supporting information Text S3).

2.2.3 | Polynomial regression analysis

Polynomial regressions with 99% confidence intervals were fit through these coordinates for the protoconid (POL-PR). These regressions and their correlations were performed in R Commander, by running the package *ggplot2* and exporting the figures in a vector format (.pdf). The final number of degrees of the polynomial regression was established when four decimals of the adjusted R-squared start repeating when the degrees of the polynomial regression are progressively increased.

2.3 | Validation of the new methodology

2.3.1 | Subsamples

The sample is composed of 26 lower molars. They were randomly divided in two subsamples using the function *sample* available in R. The validation subsample consisted of five molars (2 M1s and 3 M2s) as it is recommended this subsample be comprised of 10% of the parent sample (Alreck & Settle, 2003). The second subsample ($n = 21$) was used to generate the polynomial regression. POL-PR was therefore analyzed using 1,071 points (21 molars × 51 points/molars). We also evaluated whether $n = 21$ molars was sufficiently high to get a polynomial regression that resists the addition/removal of molars without modifying its curvature.

2.3.2 | Digital wear simulation and reconstruction

The validation subsample of five molars was digitally worn using the open-source software GIMP 2.8. The simulated wear consisted of removing all the enamel that was above the horizontal line that crosses over the dentine horn of the protoconid.

Each molar was reconstructed using the polynomial regression POL-PR. A detailed description of how to automatically place the regression plot over the worn tooth can be read in SOM Text S4, but see also SOM Video S1. Protoconid occlusal outlines were also reconstructed following the instructions in Guatelli-Steinberg and Reid (2008) and Smith, Martin, and Leakey (2003), and Smith et al. (2006a, 2009, 2012) (Methods 1 and 2, respectively). The former study follows the contour of each side of the tooth cusp, projecting them proximally until both sides met, while the latter studies reconstruct the molars based on the profiles of unworn teeth. Concerning Method 2, as they reconstruct worn teeth using an unworn tooth of the same tooth type, we selected one random M1 and one random M2 from the subsample

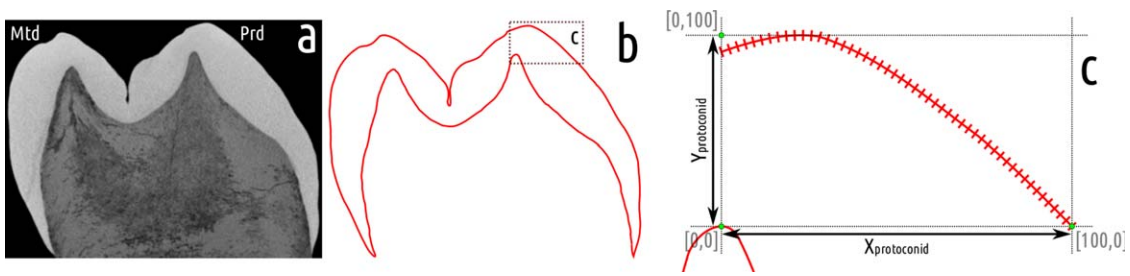

FIGURE 2 Raster-to-vector conversion of the reference plane and division of the enamel contour in segments. (a) Microtomographic reference plane of a M_2. Mtd = Metaconid; Prd = Protoconid. (b) Vector graphic of the enamel contour using Inkscape 0.91. (c) *Xprotoconid* and *Yprotoconid* define the region of the protoconid divided in 50 segments (51 points at equal distances). It is used to perform the polynomial regression POL-PR

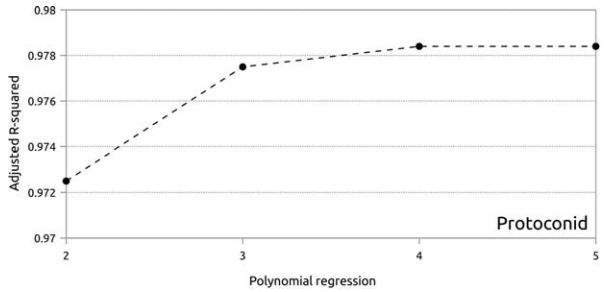

FIGURE 3 Variation of adjusted R-squared depending on the degrees of the polynomial regression equation used to obtain POL-PR

of 21 molars to reconstruct either the M1s or the M2s that were digitally worn.

2.3.3 | Variables and interobserver error

We measured the cuspal enamel thickness of the protoconid (CET) and the crown height of the protoconid (CH) in the reconstructed teeth. Then, we compared the real value of the original image of the teeth with the values obtained after using the different reconstruction methods (POL-PR, Methods 1 and 2).

For CET, we estimated the location of the first perikyma in nine molars of this study. The first perikyma was placed on average at 9.43° from the cusp tip of the protoconid distally (toward the cervix) (supporting information Text S5 and Figure S1).

The validation process was carried out in each tooth by four coauthors of this study (CG, LMF, YQ, RG), who measured the two variables (CET, CH) in the validation subsample of five molars using the three methods of reconstruction (POL-PR, Method 1, Method 2) and they also measured the original variables in the unworn microCT planes. Interobserver error was also evaluated.

2.4 | Comparison of the polynomial regressions of M1 + M2 vs. M1/M2

One important question is whether or not the polynomial regression of both lower molars (M1 + M2) is more accurate when estimating CET and CH, instead of performing separate regressions for each tooth type. For this purpose, we divided the two subsamples per molar type. On the one hand, we obtained the eight M1s to perform the polynomial regression that was employed to reconstruct the protoconid of the two remaining M1s of the validation sample. On the other hand, 13 M2s were used to get the polynomial regression that will be used to reconstruct the remaining three M2s. Two coauthors measured the estimated and real values of CET and CH (MM-M, CG).

3 | RESULTS

The subsample of $n = 21$ molars was used to calculate the polynomial regression POL-PR. This is a 4th degree polynomial regression, with $P < .0000$ and adjusted R-squared = 0.9784) (supporting information Table S1 and Figure 3). Figure 3 represents the change of the adjusted R-squared depending of the degrees of the polynomial regression.

To evaluate whether the subsample of 21 molars comprises a sufficiently high number of molars to generate a polynomial regression that remain unmodified with the inclusion/removal of new molars, we randomly assigned one number (1–21) to each molar. We then generated 21 polynomial regressions, consecutively adding one molar per regression and observing its effect on the curves. We repeated this process for the 8 M1s and the 13 M2s separately. All these regressions are represented in Figure 4. A common pattern observed in all regressions in that the curves tend to stabilize as the number of molars in the polynomial regressions increases. In the case of the M1s, after the 6th molar the curve tends to be stable at the points where CH and CET are

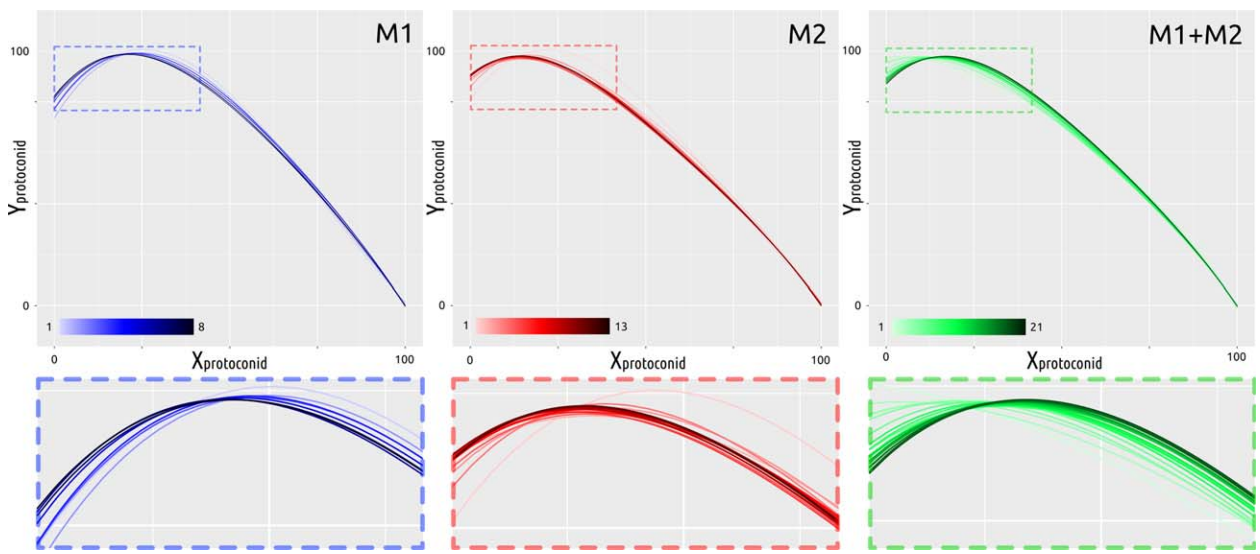

FIGURE 4 The curvature of the polynomial regression becomes more stable as the number of molars increases in the combined sample of M1 and M2 (right, green), and also in the curvatures for the M1 (left, blue) and M2 (center, red) separately. A detailed section of each group can be seen below the complete charts. In all parts of the figure, the darker the colour of the scale is, the more number of molars are included in the polynomial regression

measured. This occurs after the 9th molar in the M2s and after the 16th molar in the mixed sample. Looking at the last three polynomial regressions (the ones that represent 19, 20, and 21 molars), we observe that their patterns of curvature are identical and indistinguishable. This means that POL-PR is resistant to significant changes of its curvature with $n = 21$ molars, which implies that it can be used as a model to test its usefulness when reconstructing the morphology of the protoconid.

Table 2 shows the descriptive statistics of the interobserver error of both CET and CH variables, including means and standard deviations of estimated and real values per molar. This data evidences the differences that are present when comparing different reconstruction methodologies. POL-PR presents less standard deviation values than the other two methodologies in both CET and CH, with the exception of CET (M3) and CH (M1). In these two cases, the standard deviations between POL-PR and the closest methodology are very narrow. The differences between the mean of the real values and the means of the reconstruction methodologies exhibit that POL-PR best reconstruct three out of five molars for both CET and CH variables.

Shapiro-Wilk tests were performed to test normality distribution for both variables (CET and CH) and molars (Table 2). Except for POL-PR (M2) and Real (M1) that were nonnormal distributed ($P < .05$), the remaining variables and molars resulted to be normal distributed. We also tested equality of variances by performing Fisher tests two by two (Table 3). These tests demonstrate that POL-PR values compared to their real ones present the same variance ($P > .05$) in all molars. This fact also occurs for the Method 2 but it is not the case for Method 1, where some comparisons don't have the same variance as CET (M1, M2, M4) and CH (M2).

The interobserver error and the average percentage error between the real/estimated values of the variables (CET and CH) are represented in Figure 5. Percentage error has been calculated by applying this formula: [(mean_Method_X−mean_Real) * 100/mean_Real]. Depending on the results of previous statistical tests (Shapiro-Wilk and

TABLE 2 Interobserver error descriptive statistics of CET and CH variables. Real measures and their estimates using the three reconstruction methodologies (POL-PR, Methods 1 and 2) over the five molars of the validation subsample are shown (M1–M5). Means and standard deviations (*sd*) were calculated, as well as *diff* [mean(POL-PR/Method 1/Method 2) – mean (Real)] and *%error* [(mean(POL-PR/Method 1/Method 2) – mean(Real)) * 100/mean(Real)]. To evaluate normality distribution, Shapiro-Wilk tests (W) were applied, marking with an asterisk (*) significant *P*-values ($P < .05$). Sample size in each row is $n = 4$.

		Descriptive statistics								Normality test			
		CET				CH				CET		CH	
		mean	sd	diff	%error	mean	sd	diff	%error	W	*P*-value	W	*P*-value
M1	Real	1.35	0.04	–	–	7.83	0.41	–	–	0.8299	.1675	0.7436	0.0336*
	POL-PR	1.39	0.04	0.04	+2.66	7.94	0.20	0.11	+1.40	0.9256	.5688	0.7625	0.0502
	Method 1	1.56	0.25	0.21	+15.32	8.17	0.35	0.35	+4.40	0.9758	.8769	0.7675	0.0555
	Method 2	1.45	0.11	0.10	+7.39	7.95	0.17	0.12	+1.52	0.9107	.4863	0.9980	0.9937
M2	Real	1.82	0.04	–	–	8.03	0.09	–	–	0.9317	.6046	0.9323	0.6079
	POL-PR	1.74	0.06	−0.07	−4.07	7.60	0.11	−0.43	−5.30	0.6574	.0033*	0.8314	0.1714
	Method 1	1.97	0.50	0.15	+8.51	8.51	0.92	0.48	+6.00	0.9528	.7338	0.9400	0.6544
	Method 2	1.47	0.10	−0.35	−19.30	7.34	0.20	−0.69	−8.60	0.9667	.8212	0.8768	0.3253
M3	Real	1.08	0.06	–	–	7.83	0.22	–	–	0.9226	.5517	0.9165	0.5173
	POL-PR	1.31	0.10	0.23	+21.38	7.88	0.23	0.05	+0.67	0.9424	.6688	0.9491	0.7104
	Method 1	1.33	0.08	0.24	+22.42	7.90	0.37	0.08	+0.97	0.9124	.4952	0.9024	0.4428
	Method 2	1.07	0.12	−0.02	−1.43	7.38	0.26	−0.45	−5.76	0.9047	.4548	0.8593	0.2576
M4	Real	1.45	0.08	–	–	7.95	0.19	–	–	0.8280	.1626	0.9111	0.4882
	POL-PR	1.27	0.06	−0.18	−12.28	7.48	0.15	−0.47	−5.92	0.9958	.9847	0.9039	0.4509
	Method 1	1.57	0.58	0.12	+8.50	7.83	0.60	−0.12	−1.52	0.9819	.9132	0.9867	0.9399
	Method 2	1.21	0.22	−0.24	−16.54	7.64	0.29	−0.30	−3.80	0.9940	.9769	0.9464	0.6935
M5	Real	1.77	0.06	–	–	8.93	0.14	–	–	0.8162	.1347	0.7739	0.0631
	POL-PR	1.59	0.07	−0.18	−10.07	8.38	0.13	−0.55	−6.20	0.9007	.4347	0.9638	0.8027
	Method 1	1.95	0.29	0.18	+10.26	8.72	0.51	−0.21	−2.39	0.9725	.8571	0.9848	0.9293
	Method 2	1.56	0.20	−0.21	−11.76	8.53	0.13	−0.40	−4.47	0.9533	.7368	0.7913	0.0875

TABLE 3 Statistical tests and *P*-values to compare equality of variances (Fisher tests) and equality of means/medians (*t*-tests, Welch tests and Mann-Whitney tests, represented as t/Welch/MW) performed between real measurements of CET and CH and their estimates employing the three reconstruction methodologies (POL-PR, Methods 1 and 2). These tests were applied for every molar of the validation subsample (M1-M5). Significant statistical differences ($P < .05$) have been pointed out by using the asterisk symbol (*). Sample size in all tests was $n = 4$. F and *W/t* represents the value of the functions. *T*-tests were mainly applied, but (a) and (b) indicates that Welch tests and Mann-Whitney tests were employed, respectively

		Real			
		Fisher		t/Welch/MW	
CET		*F*	*P-value*	*W/t*	*P-value*
M1	POL-PR	1.0468	.9709	1.3896	0.2140
	Method 1	47.9320	.0099*	1.6362[a]	0.1967
	Method 2	0.1122	.1054	−1.7540	0.1300
M2	POL-PR	2.1162	.5539	2.0000[b]	0.1102
	Method 1	130.5600	.0022*	0.6113[a]	0.5836
	Method 2	0.1949	.2124	6.4187	0.0007*
M3	POL-PR	3.2273	.3616	4.0729	0.0066*
	Method 1	2.2073	.5323	4.9031	0.0027*
	Method 2	0.2123	.2354	0.2347	0.8223
M4	POL-PR	0.5108	.5951	−3.6485	0.0107*
	Method 1	54.0790	.0083*	0.4184[a]	0.7029
	Method 2	0.1262	.1230	2.0220	0.0897
M5	POL-PR	1.3575	.8076	−3.6805	0.0103*
	Method 1	20.8030	.0329*	1.2340[a]	0.2980
	Method 2	0.0951	.0846	1.9467	0.0990
CH					
M1	POL-PR	0.2420	.2743	7.0000[b]	0.8857
	Method 1	0.7228	.7960	13.0000[b]	0.2000
	Method 2	6.2123	.1678	8.0000[b]	1.0000
M2	POL-PR	1.4548	.7655	−5.9639	0.0010*
	Method 1	102.7600	.0032*	1.0381[a]	0.3742
	Method 2	0.2052	.2260	6.2528	0.0008*
M3	POL-PR	1.1353	.9194	0.3317	0.7514
	Method 1	2.9899	.3924	0.3541	0.7354
	Method 2	0.6955	.7725	2.6791	0.0366*
M4	POL-PR	0.5920	.6773	−3.9145	0.0079*
	Method 1	10.0420	.0900	−0.3809	0.7164
	Method 2	0.4331	.5098	1.7438	0.1318
M5	POL-PR	0.9646	.9770	−5.8081	0.0011*
	Method 1	13.9430	.0576	−0.8129	0.4473
	Method 2	1.1052	.9364	4.2475	0.0054*

Fisher), new statistical tests were carried out to compare means/medians in all molars between real and estimated values in both CET and CH variables. Thus, Welch tests, Mann-Whitney tests and *t* tests were applied accordingly (Table 3). All reconstruction methodologies display significant statistical differences in some variables and molars when they are compared to the real values. Due to POL-PR is characterized by narrower standard deviations respect to the other methods, it is understandable that slightly over- and underestimates would imply statistical significant differences in their means/medians. Moreover, the probability of finding statistically nonsignificant differences increases when the variance is wider (as is the case of Methods 1 and 2).

Combining all five molars of the validation subsample, the average percentage error for the methods based on the polynomial regression (POL-PR) is shown in Table 4. CET tends to be −2.17 underestimated using POL-PR, with a 95% confidence interval of −4.60% and 0.74%. CH tends to be underestimated by −3.18% using POL-PR, with a confidence interval of −3.77% and −2.54%.

The polynomial regressions and associated prediction intervals for M1s and M2s can be seen in Figure 6. There is a high degree of overlap between molar positions. M2s acquire its maximum crown height in a slightly more buccal position compared to the same point in M1s. Crown heights and cuspal enamel thicknesses of the validation subsample have been measured depending on their molar position. Percentage errors between real and estimated measurements of CET and CH can be seen in Table 5. Applying the polynomial regression of the M1 to the two M1s of the validation subsample, the mean percentage error in respect of their real values in CET is −9.48%. Applying the same protocol to the M2s yields a value of +4.11%. For crown heights, these values are −3.88% and −2.52% for the M1s and M2s, respectively.

Our results indicate that molar-specific polynomial regressions applied separately to M1s and M2s do not considerably improve the estimates obtained from the regression equation made by combining M1s and M2s. For instance, mean percentage error using the latter regression for CET is −2.17%, which is a lower percentage error than the values from the molar-specific regressions. In CH these differences are minimal, as the mean percentage error is −3.18% using the polynomial regression of both molars, and −3.88 and −2.52 using the regression equation of the M1s and M2s, respectively. We have therefore considered the regression that is formed by merging both molars as the best proxy to estimate CET and CH in both M1s and M2s.

4 | DISCUSSION

In paleoanthropology, fossil teeth with complete and unworn crowns are relatively scarce. However, these teeth are extremely valuable for studies of either the external morphology (Gómez-Robles et al., 2008; Gómez-Robles, de Bermúdez de Castro, Martinón-Torres, & Prado-Simón, 2011a; Gómez-Robles, Martinón-Torres, Bermúdez de Castro, Prado-Simón, & Arsuaga, 2011b; Martinón-Torres, Bermúdez de Castro, Gómez-Robles, Prado-Simón, & Arsuaga, 2012; Martinón-Torres

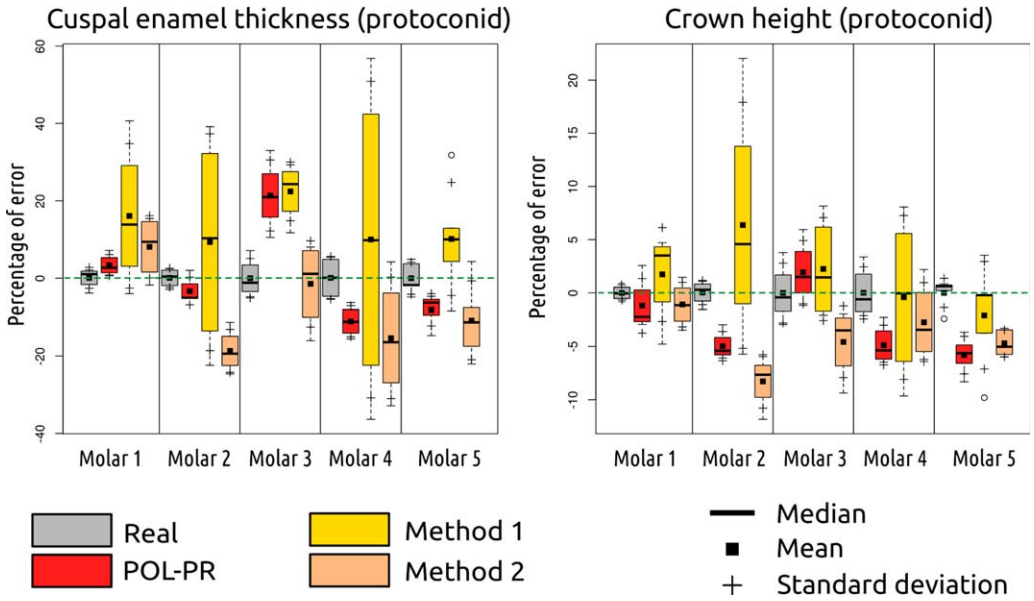

FIGURE 5 Box and whisker chart of the percentage error estimated by four coauthors for each variable and molar of the validation subsample ($n = 5$). The three methodologies described in the text (POL-PR, Method 1, Method 2) were used to reconstruct the contour of the protoconid enamel surface

et al., 2006) or the internal morphology of molar teeth (Martínez de Pinillos et al., 2014; Martinón-Torres et al., 2014). Nondestructive methods, either synchrotron or microcomputed tomography are capable of taking very accurate 2-D and 3-D measurements of teeth in comparison to physical sections (Kono, 2004; Olejniczak, Tafforeau, Feeney, & Martin, 2008b).

In order to measure many dental variables in worn teeth (such as cuspal enamel thickness, crown height, relative enamel thickness, etc.) a reconstruction of the missing parts is required. Therefore, the accuracy of the method employed to make the reconstructions is very important as it can over- or underestimate the measurements, which can in turn lead to taxonomic, phylogenetic, physiological and age-at-death misclassifications (Dean & Reid, 2001; Guatelli-Steinberg & Reid, 2008; Guatelli-Steinberg, Reid, & Bishop, 2007; Lacruz & Bromage, 2006; Lacruz, Rozzi, & Bromage, 2006; Martin, 1983, 1985; Reid et al., 2008; Smith et al., 2006a,b, 2010; Suwa & Kono, 2005).

Here we have developed a new methodology based on polynomial regression equations to accurately reconstruct worn molars cusps. The polynomial regression to reconstruct the protoconid of lower molars, POL-PR, is employed to estimate cuspal enamel thickness and crown height of the protoconid. Not only are these variables more accurately measured, but also other variables that depend on them might be improved, such as enamel formation times and enamel extension rates (Dean, 2009; Dean & Reid, 2001; Guatelli-Steinberg & Reid, 2008; Guatelli-Steinberg, Floyd, Dean, & Reid, 2012; Lacruz, 2007; Lacruz, Dean, Ramirez-Rozzi, & Bromage, 2008; Reid & Dean, 2006; Smith et al., 2010). In order to evaluate the accuracy of our methodology, we also reconstructed the same teeth applying the methods previously described by other authors.

The results demonstrate that the new methodology described here shows less interobserver variation than the two previously described methods, whose procedures remain unvalidated (Guatelli-Steinberg & Reid, 2008; Reid & Dean, 2006; Smith et al., 2012).

TABLE 4 Means of the percentage errors (%) of each variable (CET and CH) employing the three reconstruction methodologies (POL-PR, Methods 1 and 2)

	POL-PR	Method 1	Method 2
CET	−2.17	+12.17	−9.56
CH	−3.18	+1.40	−4.25

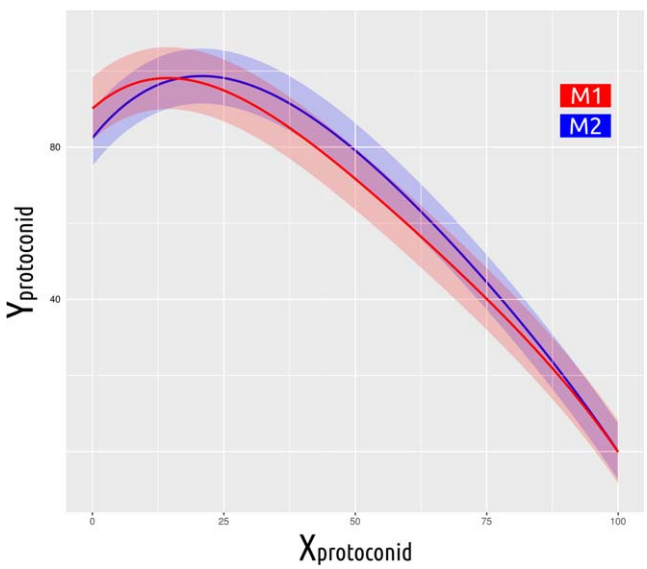

FIGURE 6 Polynomial regressions for the M1s (red) and M2s (blue)

TABLE 5 Percentage Errors (%) of Real Crown Heights (CH) and Cuspal Enamel Thicknesses (CET) Their Respective Estimates Using the Molar-Specific Polynomial Regressions (M1s or M2s)

	M1 polynomial regression		M2 polynomial regression		
	Molar 3 (M1)	Molar 4 (M1)	Molar 1 (M2)	Molar 2 (M2)	Molar 5 (M2)
CET	+8.38	−22.81	+7.93	+4.11	+1.19
CH	−0.65	−7.07	+0.88	−4.27	−3.92
Mean CET	−9.48		+4.11		
Mean CH	−3.88		−2.52		

The methodology that displays the highest degree of interobserver variation is that described as Method 1. The fact that these values are so different from what is termed by us as Method 2 is because the latter involves the real contour of a tooth and the former does not. However, both of these methods involve high degrees of subjectivity. In some particular cases, we observed that the measurements obtained through these methodologies fit better with the real value compared with those obtained using the polynomial regression equations. However, the interobserver variation in these methodologies is very wide, and so obtaining such apparently good estimates might well be explained by random and arbitrary effects. It is highly likely that the dispersion and variance of the measurements were different with the inclusion of new observers in the estimation of these variables. Compared to the interobserver error apparent when using the methodologies described by Methods 1 and 2, our own methodology shows the lowest variation and the results also fall closer to the known values. The polynomial regression equations generated here are an attempt to establish for the first time a new methodology where the procedure for reconstructing worn tooth is standardized and comparable.

A further point to note is that the interobserver variation documented using the polynomial regression equation described here is not statistically different to the interobserver variation of the real measurements made from the unworn teeth. This suggests that the new methodology is highly uniform and homogeneous, and is easily reproducible by researchers/observers. When reconstructing these dental variables using this new methodology, we recommend also calculating the 95% confidence intervals and/or prediction intervals. Hence, in each of these ways we feel our method significantly improves upon previous methods when reconstructing specific important dental variables affected by cuspal wear.

Although the estimations of CET and CH using POL-PR are valuable, we acknowledge that more *H. sapiens* teeth are necessary to extend its validity. Furthermore, it has also been stated that differences exist in the enamel thickness in different populations from all around the globe and among hominin species (Grine, 2005; Olejniczak et al., 2008a; Smith et al., 2012; Suwa & Kono, 2005). To what extent the inclusion of different populations of modern humans affects the polynomial regression remains unknown. More studies should be focused on this issue, as the knowledge of the protoconid morphology and how it varies from one population/species to another that together offer an unique opportunity to improve this methodology.

Reconstructing crown heights accurately might be useful to estimate the percentage of enamel that has been lost. Their respective worn deciles and perikymata number can therefore be evaluated. As the first deciles of the crown height, which correspond to the ones that are closer to the cusp tip of the enamel, present lower number of perikymata counts compared to the most cervical deciles (Dean & Reid, 2001; Guatelli-Steinberg & Reid, 2008; Reid & Dean, 2006), we would expect this new methodology to be sufficiently capable of significantly reducing the range of variation of crown formation times in slightly worn molars. However, we acknowledge that its validity in assessing the total number of perikymata and crown formation times must be quantified in future studies.

In conclusion, this new methodology designed to reconstruct slightly worn lower permanent molars has clear advantages over other methods. First, it is easily reproducible, allowing an increasing numbers of teeth to be included in studies of dental development with greater confidence. Second, it shows a high degree of accuracy when reconstructing the contours of worn cuspal enamel. Third, associated estimation errors can be determined. Fourth, it can be used for both M1 and M2 lower molars of *H. sapiens*. Fifth, the new estimates would be comparable among different authors following this methodology. Sixth, it uses mainly open-source software. Seventh, it greatly reduces the operator-dependent procedures in order to drastically reduce the bias.

ACKNOWLEDGMENTS

This research was supported with funding from the Dirección General de Investigación of the Spanish Ministerio de Educación y Ciencia (MEC) and Spanish Ministerio de Economía y Competitividad (MINECO), Project No. CGL2012-38434-C03-01/02/03, CGL2015-65387-C3-3-P, and 2014 SGR 900 Group of Analyses on Socio-ecological Processes, Cultural Changes and Population dynamics during Prehistory (GAPS) of the Generalitat de Catalunya. We also express thanks for the support of Acción Integrada España Francia (HF2007-0115); Consejería de Educación de Junta de Castilla y León (CEN074A12-2) and The Leakey Foundation through the personal support of Gordon Getty (2013) and Dub Crook (2014, 2015) to one of the authors (MM-T). MM, CG and MMP research has been supported by a predoctoral grant of the Junta de Castilla y León (BOCYL-D-30122013-33 and BOCYL-D-20052013-14) cofinanced by European Social Funds through the Consejería de Educación, and economic support by the Atapuerca Foundation. LMF has

a Post-Doctoral Grant from the Fundación Atapuerca. Acknowledgement to the Cáceres Museum and Extremadura Government for their permission to study Maltravieso materials, as well as to José Miguel Carretero. Without the remarkable participation of the Atapuerca and EPPEX teams, this work would have never been possible to carry through. We want also to express our gratitude to Cova dels Galls Carboners and Cova de la Guineu excavation teams. The mCT scanner of the dental collection was performed in the Microscopy Laboratory at CENIEH facilities. We are especially grateful to the referees and the Associated Editor for their comments and suggestions, which have greatly improved the paper. The Cova de la Guineu excavation is funded by the 2014/100482 project of the Culture Department of the Generalitat de Catalunya and by the AGAUR project 2014SGR-108 and MINECO HAR2014-55131. The Galls Carboners excavation is funded by the 2014/100574 project of the Culture Department of the Generalitat de Catalunya.

REFERENCES

Alreck, P. L., & Settle, R. B. (2003). *The survey research handbook* (3rd ed.). Boston: McGraw-Hill Education.

Benazzi, S., Panetta, D., Fornai, C., Toussaint, M., Gruppioni, G., & Hublin, J.-J. (2014). Technical Note: Guidelines for the digital computation of 2D and 3D enamel thickness in hominoid teeth. *American Journal of Physical Anthropology*, *153*, 305–313.

Callejo, S. C. (1958). *La cueva prehistórica del maltravieso, junto a cáceres*. Cáceres: Publicaciones de la Biblioteca Pública de la Ciudad.

Carbonell, E., Canals, A., Sauceda, I., Barrero, N., Carbajo, Á., Díaz, Ó., … Falguères, C. (2005). La grotte de Santa Ana (Cáceres, Espagne) et l'évolution technologique au Pléistocène dans la Péninsule ibérique. *L'Anthropologie*, *109*, 267–285.

Cerrillo, C. E., & González, C. A. (2007). *Cuevas para la eternidad: sepulcros prehistóricos de la provincia de cáceres*. Mérida: Asamblea de Extremadura.

Dean, C. (2009). Extension rates and growth in tooth height of modern human and fossil hominin canines and molars. In T. Koppe, G. Meyer, K. W. Alt, A. Brook, M. C. Dean, I. Kjaer, J. R. Lukacs, B. H. Smith, M. F. Teaford (Eds.), *Frontiers of oral biology* (Vol. *13*, pp. 68–73). Basel: KARGER.

Dean, M. C., & Reid, D. J. (2001). Perikymata spacing and distribution on hominid anterior teeth. *American Journal of Physical Anthropology*, *116*, 209–215.

Dean, C., Leakey, M. G., Reid, D., Schrenk, F., Schwartz, G. T., Stringer, C., & Walker, A. (2001). Growth processes in teeth distinguish modern humans from Homo erectus and earlier hominins. *Nature*, *414*, 628–631.

FitzGerald, C. M., & Rose, J. C. (2008). Reading between the lines: Dental development and subadult age assessment using the microstructural growth markers of teeth. In M. A. Katzenberg and S. R. Saunders (Eds.), *Biological anthropology of the human skeleton* (2nd ed., pp. 237–263). New York, N. Y.: Wiley Liss.

Gómez-Robles, A., de Bermúdez de Castro, J. M., Martinón-Torres, M., & Prado-Simón, L. (2011a). Crown size and cusp proportions in Homo antecessor upper first molars. A comment on Quam et al. 2009. *Journal of Anatomy*, *218*, 258–262.

Gómez-Robles, A., Martinón-Torres, M., Bermúdez de Castro, J. M., Prado, L., Sarmiento, S., & Arsuaga, J. L. (2008). Geometric morphometric analysis of the crown morphology of the lower first premolar of hominins, with special attention to Pleistocene Homo. *Journal of Human Evolution*, *55*, 627–638.

Gómez-Robles, A., Martinón-Torres, M., Bermúdez de Castro, J. M., Prado-Simón, L., & Arsuaga, J. L. (2011b). A geometric morphometric analysis of hominin upper premolars. Shape variation and morphological integration. *Journal of Human Evolution*, *61*, 688–702.

Gómez-Sánchez, D., Olalde, I., Pierini, F., Matas-Lalueza, L., Gigli, E., Lari, M., … Lalueza-Fox, C. (2014). Mitochondrial DNA from El Mirador Cave (Atapuerca, Spain) reveals the heterogeneity of chalcolithic populations. *PLoS ONE*, *9*, e105105.

Grine, F. E. (2005). Enamel thickness of deciduous and permanent molars in modern *Homo sapiens*. *American Journal of Physical Anthropology*, *126*, 14–31.

Guatelli-Steinberg, D., & Reid, D. J. (2008). What molars contribute to an emerging understanding of lateral enamel formation in Neandertals vs. modern humans. *Journal of Human Evolution*, *54*, 236–250.

Guatelli-Steinberg, D., Floyd, B. A., Dean, M. C., & Reid, D. J. (2012). Enamel extension rate patterns in modern human teeth: Two approaches designed to establish an integrated comparative context for fossil primates. *Journal of Human Evolution*, *63*, 475–486.

Guatelli-Steinberg, D., Reid, D. J., & Bishop, T. A. (2007). Did the lateral enamel of Neandertal anterior teeth grow differently from that of modern humans?. *Journal of Human Evolution*, *52*, 72–84.

Hillson, S. (1996). *Dental anthropology*. Cambridge: Cambridge University Press.

Kono, R. T. (2004). Molar enamel thickness and distribution patterns in extant great apes and humans: New insights based on a 3-dimensional whole crown perspective. *Anthropological Science*, *112*, 121–146.

Kono, R. T., & Suwa, G. (2005). Effects of molar crown orientation to measures of lateral enamel thickness in the mesial cusp section. *Bulletin of the National Science Museum. Series B*, *31*, 11–22.

Lacruz, R. S. (2007). Enamel microstructure of the hominid KB 5223 from Kromdraai, South Africa. *American Journal of Physical Anthropology*, *132*, 175–182.

Lacruz, R. S., & Bromage, T. G. (2006). Appositional enamel growth in molars of South African fossil hominids. *Journal of Anatomy*, *209*, 13–20.

Lacruz, R. S., Dean, M. C., Ramirez-Rozzi, F., & Bromage, T. G. (2008). Megadontia, striae periodicity and patterns of enamel secretion in Plio-Pleistocene fossil hominins. *Journal of Anatomy*, *213*, 148–158.

Lacruz, R. S., Rozzi, F. R., & Bromage, T. G. (2006). Variation in enamel development of South African fossil hominids. *Journal of Human Evolution*, *51*, 580–590.

Macchiarelli, R., Bondioli, L., Debénath, A., Mazurier, A., Tournepiche, J.-F., Birch, W., & Dean, M. C. (2006). How Neanderthal molar teeth grew. *Nature*, *444*, 748–751.

Mahoney, P. (2008). Intraspecific variation in M1 enamel development in modern humans: Implications for human evolution. *Journal of Human Evolution*, *55*, 131–147.

Martin, L. (1985). Significance of enamel thickness in hominid evolution. *Nature*, *314*, 260–263.

Martin, L. B. (1983). *The relationships of the later miocene hominoidea*. London: University College London.

Martínez de Pinillos, M., Martinón-Torres, M., Skinner, M. M., Arsuaga, J. L., Gracia-Téllez, A., Martínez, I., … Bermúdez de Castro, J. M. (2014). Trigonid crests expression in Atapuerca-Sima de los Huesos lower molars: Internal and external morphological expression and evolutionary inferences. *Comptes Rendus Palevol*, *13*, 205–221.

Martinón-Torres, M., Bastir, M., Bermúdez de Castro, J. M., Gómez, A., Sarmiento, S., Muela, A., & Arsuaga, J. L. (2006). Hominin lower second premolar morphology: Evolutionary inferences through geometric morphometric analysis. *Journal of Human Evolution*, *50*, 523–533.

Martinón-Torres, M., Bermúdez de Castro, J. M., Gómez-Robles, A., Prado-Simón, L., & Arsuaga, J. L. (2012). Morphological description and comparison of the dental remains from Atapuerca-Sima de los Huesos site (Spain). *Journal of Human Evolution*, *62*, 7–58.

Martinón-Torres, M., Martínez de Pinillos, M., Skinner, M. M., Martín-Francés, L., Gracia-Téllez, A., Martínez, I., … Bermúdez de Castro, J. M. (2014). Talonid crests expression at the enamel–dentine junction of hominin lower permanent and deciduous molars. *Comptes Rendus Palevol*, *13*, 223–234.

Molnar, S. (1971). Human tooth wear, tooth function and cultural variability. *American Journal of Physical Anthropology*, *34*, 175–190.

Morales, J. I., Cebrià, A., Mestres, J., Oms, F. X., & Allué, E. (2013). La Cova de la Guineu. 12.000 anys de presència humana a les capçaleres del Foix. III Monogr Foix:172–183.

Muñoz, L., & Canals, A. (2008). Nuevos restos humanos hallados en la cueva de Maltravieso. In P. Sanabria Marcos (Ed). *El mensaje de maltravieso 50 años después (1956–2006)* (Vol. *8*, pp. 205–207). Cáceres: Museo Provincial de Cáceres.

Nanci, A. (2007). *Ten cate's oral histology: Development, structure, and function* (7th ed.), St. Louis, MO: Mosby.

Olejniczak, A. J., & Grine, F. E. (2006). Assessment of the accuracy of dental enamel thickness measurements using microfocal X-ray computed tomography. *The Anatomical Record. Part A, Discoveries in Molecular, Cellular, and Evolutionary Biology*, *288A*, 263–275.

Olejniczak, A. J., Gilbert, C. C., Martin, L. B., Smith, T. M., Ulhaas, L., & Grine, F. E. (2007). Morphology of the enamel-dentine junction in sections of anthropoid primate maxillary molars. *Journal of Human Evolution*, *53*, 292–301.

Olejniczak, A. J., Smith, T. M., Skinner, M. M., Grine, F. E., Feeney, R. N. M., Thackeray, J. F., & Hublin, J. J. (2008a). Three-dimensional molar enamel distribution and thickness in Australopithecus and Paranthropus. *Biological Letters*, *4*, 406–410.

Olejniczak, A. J., Tafforeau, P., Feeney, R. N. M., & Martin, L. B. (2008b). Three-dimensional primate molar enamel thickness. *Journal of Human Evolution*, *54*, 187–195.

Reid, D. J., & Dean, M. C. (2006). Variation in modern human enamel formation times. *Journal of Human Evolution*, *50*, 329–346.

Reid, D. J., Guatelli-Steinberg, D., & Walton, P. (2008). Variation in modern human premolar enamel formation times: Implications for Neandertals. *Journal of Human Evolution*, *54*, 225–235.

Saunders, S. R., Chan, A. H. W., Kahlon, B., Kluge, H. F., & FitzGerald, C. M. (2007). Sexual dimorphism of the dental tissues in human permanent mandibular canines and third premolars. *American Journal of Physical Anthropology*, *133*, 735–740.

Smith, T. M., Martin, L. B., & Leakey, M. G. (2003). Enamel thickness, microstructure and development in *Afropithecus turkanensis*. *Journal of Human Evolution*, *44*, 283–306.

Smith, T. M., Olejniczak, A. J., Kupczik, K., Lazzari, V., De Vos, J., Kullmer, O., … Tafforeau, P. (2009). Taxonomic assessment of the Trinil molars using non-destructive 3D structural and development analysis. *PaleoAnthropology*, *2009*, 117–129.

Smith, T. M., Olejniczak, A. J., Tafforeau, P., Reid, D. J., Grine, F. E., & Hublin, J. (2006a). Molar crown thickness, volume, and development in South African Middle Stone Age humans. *South African Journal of Science*, *102*, 513.

Smith, T. M., Olejniczak, A. J., Zermeno, J. P., Tafforeau, P., Skinner, M. M., Hoffmann, A., … Hublin, J.-J. (2012). Variation in enamel thickness within the genus Homo. *Journal of Human Evolution*, *62*, 395–411.

Smith, T. M., Reid, D. J., & Sirianni, J. E. (2006b). The accuracy of histological assessments of dental development and age at death. *Journal of Anatomy*, *208*, 125–138.

Smith, T. M., Tafforeau, P., Reid, D. J., Pouech, J., Lazzari, V., Zermeno, J. P., … Hublin, J.-J. (2010). Dental evidence for ontogenetic differences between modern humans and Neanderthals. *Proceedings of the National Academy of Sciences of the United States of America*, *107*, 20923–20928.

Suwa, G., & Kono, R. T. (2005). A micro-CT based study of linear enamel thickness in the mesial cusp section of human molars: Reevaluation of methodology and assessment of within-tooth, serial, and individual variation. *Anthropological Science*, *113*, 273–289.

Xing, S., Martinón-Torres, M., Bermúdez de Castro, J. M., Wu, X., & Liu, W. (2015). Hominin teeth from the early Late Pleistocene site of Xujiayao, Northern China. *American Journal of Physical Anthropology*, *156*, 224–240.

SUPPORTING INFORMATION

Additional Supporting Information may be found in the online version of this article.

SOM Table S1. Regression equations based on 21 molars to reconstruct the upper part of the enamel (POL-PR).

SOM Figure S1. (Above) Isosurface of one molar (6.0.0). The horizontal green line represents the plane of reference (see main text for further details). The red vertical line indicates the position of the first perikyma. (Below) Graphic definition of the angle between the enamel tip, the first perikyma (red point) and dentine horn tip.

SOM Figure S2. Polynomial regression and 99% confidence interval of POL-PR. It is based on the contour of 21 molars. Vertical blue line represents maximum heights. Relative coordinates are represented in their own corners.

SOM Video S1. Visual representation in Inkscape of how to reconstruct the protoconid enamel using the POL-PR polynomial regression equation. The vector graphic is SOM Figure S2, which is in PDF format. Spreadsheet is SOM Excel S1.

How to cite this article: Modesto-Mata M, García-Campos C, Martín-Francés L, et al. New methodology to reconstruct in 2-D the cuspal enamel of modern human lower molars. *Am J Phys Anthropol*. 2017;163:824-834. https://doi.org/10.1002/ajpa.23243